[5] P. L. Overfelt, *Superspheroid Geometries for Radome Analysis*. China Lake, CA: Naval Air Warfare Center Weapons Division, Technical Publication 8216, Aug. 1994.
[6] ——, *Computer Codes for Electromagnetic Design and Analysis of Radomes*. China Lake, CA: Naval Weapons Center, Technical Publication 6598, Mar. 1985.
[7] P. L. Overfelt, C. S. Kenney, D. J. White, and W. O. Alltop, *Radome Analysis and Design Tool (Final Report)*. China Lake, CA: Naval Air Warfare Center Weapons Division, Technical Publication 8171, Nov. 1993.
[8] P. L. Overfelt, "Two-dimensional radome modelling: A boundary perturbation approach," in *1984 IEEE Int. Symp. Dig. Antennas Propagat.*, June 1984, pp. 201–205.
[9] P. L. Overfelt and D. J. White, "Electromagnetic analysis of radomes using a spherical wave point dipole source array technique," in *21st Symp. Electromagnetic Windows Dig.*, Sept. 1988, pp. 11–25.
[10] D. C. F. Wu and R. C. Ruddock, "Plane wave spectrum-surface integration technique for radome analysis," *IEEE Trans. Antennas Propagat.*, vol. AP-22, pp. 497–500, May 1974.
[11] K. Siwiak, T. B. Dowling, and L. Lewis, "Boresight errors induced by missile radomes," *IEEE Trans. Antennas Propagat.*, vol. AP-27, pp. 832–841, Nov. 1979.
[12] J. H. Chang and K.-K. Chan, "Analysis of a two-dimensional radome of arbitrarily curved surface," *IEEE Trans. Antennas Propagat.*, vol. 38, pp. 1565–1568, Oct. 1990.
[13] X. J. Gao and L. B. Felsen, "Complex ray analysis of beam transmission through two-dimensional radomes," *IEEE Trans. Antennas Propagat.*, vol. AP-33, pp. 963–975, Sept. 1985.
[14] C. T. Tai, *Generalized Vector and Dyadic Analysis*. New York: IEEE Press, 1992.
[15] D. J. Struik, *Differential Geometry*. Cambridge, MA: Addison-Wesley, 1950.
[16] A. G. Hansen, *Similarity Analyses of Boundary Value Problems in Engineering*. Englewood Cliffs, NJ: Prentice-Hall, 1964.
[17] J. M. H. Olmsted, *Advanced Calculus*. New York: Appleton, Century, Crofts, 1961, ch. 16.
[18] M. Becker, *The Principles and Applications of Variational Methods*. Cambridge, MA: MIT Press, 1964, ch. 3.

Imaginary Part of Antenna's Admittance from its Real Part Using Bode's Integrals

Smain Amari, Martin Gimersky, and Jens Bornemann

***Abstract*— The imaginary part of an antenna input admittance is calculated from its real part using Bode's integrals. Since the real part is typically a smoother function of the frequency than the imaginary part, the procedure presented here requires computation at a smaller number of frequency points, thus saves time, and is ideal for systems whose input conductance exhibits sharp peaks. A numerical procedure to evaluate the singular Bode's integral is also presented. Numerical examples using a wire antenna are used to illustrate the advantages of this approach compared to calculations involving a densely scanned frequency range. The noise stability and robustness of the algorithm are demonstrated through the successful prediction of the susceptance and the resonant frequencies of the antenna in the presence of random noise in the conductance.**

I. Introduction

The integral relations between real and imaginary parts of response functions are widely used in quantum field theory, nuclear physics, and solid state physics. Unfortunately, this extremely useful tool does not seem to find much use in microwave engineering.

These integral relations are known under a variety of names. The Kramers–Kronig relations between the real and imaginary parts of the dielectric constants are well known to engineers and physicists. In quantum field theory and quantum many-body theory, they are sometimes known as Lehmann or spectral representations or dispersion relations [1], whereas mathematicians refer to them as Hilbert Transforms. In circuit theory, they are often called Bode's integrals, since Bode seems to have been the first to use them [2].

Kramers–Kronig relations enjoyed substantial popularity in the sixties among researchers in optics, where it is possible to measure the imaginary part since it is related to light (electromagnetic) absorption [3]. Once the imaginary part is known, these relations are used to calculate the real part. Such relations also provide a set of constraints on the moments of the functions involved as well as their asymptotic behavior and are very useful tools to check the numerical accuracy of the calculations [2], [4].

One of the most intensive numerical problems in modern antenna analysis and design is the accurate calculation of the resonant frequency, especially for antennas with sharply peaked input conductance. For such antennas, the imaginary part of the admittance oscillates violently around the resonant frequency, thereby requiring its evaluation at a very large number of frequency points in order to accurately predict the location of the resonance. Although empirically derived formulas for admittances and resonant frequencies of certain types of antennas exist, they are of low accuracy (e.g., ± 20% for helices [5]) or not known at all for other structures such as those involving anisotropic and lossy materials [6]. For all of these systems, however, the real part of the input admittance, although having sharp peaks, is much easier to describe than its imaginary part, hence requiring fewer computations around the peak which can locally be approximated by a Lorentzian.

Fortunately, it is for these numerically demanding situations that Bode's integrals will be shown to work best. Indeed, the presence of a sharp peak in the real part determines the local behavior of the imaginary part because of the singularity in the integrand. Thus it is possible to reliably predict the resonant frequency and susceptance from the real part without accurately reproducing the entire frequency dependence of the susceptance.

Since the presence of a Cauchy Principal-Value in these integral relations poses a numerical problem, which should be handled with care, a numerical procedure using cubic splines to calculate these integrals is presented. It is similar to the modified Simpson rules presented in [7] but, we feel, is more appropriate for real life quantities which are expected to be smooth functions.

The paper is organized as follows. In Section II we briefly review Bode's integrals. Section III presents a numerical procedure based on a cubic-spline interpolation to calculate the singular integrals involved. In Section IV, we apply the method to calculate the susceptance of a wire antenna as a function of frequency from its real part. The obtained results are compared with those obtained from a direct method-of-moments solution. In Section V, the noise stability of the present technique is investigated using a randomly generated error in the real part to simulate measurement errors. It is shown that the first resonant frequency is adequately predicted despite the presence of the corrupting noise.

II. Bode's Integrals

The derivation of Bode's integrals is not presented here, the reader is referred to the literature for the details [2], [3], [8]. We only

Manuscript received July 1, 1994; revised October 12, 1994.
The authors are with the Department of Electrical and Computer Engineering, University of Victoria, Victoria, B.C., Canada V8W 3P6.
IEEE Log Number 9408257.

need to stress that they apply to any *linear response* function of a physical and causal system [8]. There are situations where the presence of poles on the imaginary axis renders the relationship between the real and imaginary parts nonunique [2]. Such situations do not represent physical reality, since there are always losses in the system which eliminate such pathologies. Care must, however, be taken in determining what a response function is. The admittance of a system represents its linear response (current) to an applied voltage. The causality and linearity of the response alone guarantee that the conductance and susceptance satisfy the following integral relationships [2], [8]

$$B(\omega) = \frac{2\omega}{\pi} P \int_0^{+\infty} \frac{G(x)dx}{x^2 - \omega^2} \tag{1}$$

$$G(\omega) = G(\infty) - \frac{2}{\pi} P \int_0^{+\infty} \frac{xB(x)}{x^2 - \omega^2}. \tag{2}$$

Here P stands for the Cauchy Principal-Value, $G(\omega)$ is the input conductance and $B(\omega)$ the input susceptance. These two equations will be referred to as Bode's integrals [2].

In this paper only the first relation will be used, for the real part is much smoother than the imaginary part, thus fewer data points are needed to adequately describe it. In other areas it is usually the imaginary part that enjoys this property, which explains why it is this quantity that one calculates first. In some cases, it is also possible to measure the imaginary part, since it is related to the absorption of the incident excitation, such as optical absorption, for example.

To illustrate the usefulness of these relations, we consider a resistance R in series with a capacitance C. Without loss of generality we take the values of R and C to be unity; $R = 1$ and $C = 1$. The real and imaginary parts of the admittance of this circuit are

$$G(\omega) = \frac{\omega^2}{1 + \omega^2} \tag{3}$$

$$B(\omega) = \frac{\omega}{1 + \omega^2}. \tag{4}$$

It is straightforward to check that these two quantities satisfy Bode's integrals.

The situation we are interested in involves a real part which is numerically known on a set of frequency points. The conductance of an antenna has maxima whose sharpness is determined by the q-factor which we define as the reciprocal of the difference between the two half-amplitude points in the first peak,

$$q = \frac{1}{\Delta x}. \tag{5}$$

Here, x is a dimensionless quantity, such as the ratio of a characteristic length of the antenna (often the largest dimension) to the wavelength in free space. For large values of q, the imaginary part oscillates rapidly and changes sign around the values at which the real part peaks. Accurately describing the imaginary part in these regions from a direct solution can be numerically costly, because a large number of frequency points is needed. In the next section we present a numerical technique to evaluate the integral in (1).

III. Bode's Integrals Using Cubic Splines

This section presents a technique to numerically evaluate the Cauchy Principal-Value integral in (1). The idea is similar to the one used in deriving the modified Simpson rules in [7], except that a cubic spline is used for interpolation instead of a local second order polynomial. The use of the cubic spline guarantees the smoothness of the interpolation, as the function and its first two derivatives are required to be continuous [9], [10].

It is advantageous to split the integral in (1) into two parts, each of the following form

$$F(x) = P \int_{-\infty}^{+\infty} \frac{f(y)dy}{y - x}. \tag{6}$$

Equation (1) is consequently reduced to two integrals of the type given by this last equation, on which we now concentrate.

A popular numerical integration technique is the Legendre–Gauss quadrature, where the weights and the mesh on which the function is evaluated are chosen such that the technique is exact for polynomials up to a given order. This technique, which is well suited for functions that can be approximated by polynomials, is usually used to carry out the numerical integration in (6), often with the trick of subtracting the singularity [11]. However, such a procedure is not numerically stable for functions varying rapidly around the point x [7]. Also, the quadrature approximates the entire *integrand* $f(y)/(y - x)$ by polynomials; instead, here we only approximate the function f(y) by a cubic spline. It is much easier to accurately approximate $f(x)$ than the integrand, because of the presence of the singularity. We therefore assume that the function $f(x)$ is known at a set of points $x_i, i = 1, N$, where it has values y_i. A cubic spline is built from these points, following the standard procedure; the reader is referred to the literature for details [9], [10]. Once this is done, the integral in (6) is reduced to the sum of the contributions of each interval $[x_i, x_{i+1}]$. The result is

$$F(x) = \sum_{i=1}^{i=N} F_i(x) \tag{7}$$

where $F_i(x)$

$$\begin{aligned} F_i(x) = {} & \frac{x_{i+1}^3 - x_i^3}{18(x_{i+1} - x_i)}(z_i - z_{i+1}) - \frac{x_i + x_{i+1}}{12}\{x(z_{i+1} - z_i) \\ & + 3(x_{i-1} z_{i-1} - x_i z_{i+1})\} \\ & - \frac{1}{6(x_{i+1} - x_i)}\{(y_{i+1} - y_i)(6x + x^3) \\ & - 6x_{i+1} y_i + 6x_i y_{i+1} - x x_i^2 z_i - 3x^2 x_{i+1} z_i \\ & + 2x x_i x_{i+1} z_i + x_i^2 x_{i+1} z_i + 2x x_{i+1}^2 z_i - 2x_i x_{i-1}^2 z_i \\ & + 3x^2 x_i z_{i+1} - 2x x_i^2 z_{i+1} - 2x x_i x_{i+1} z_{i+1} + 2x_i^2 x_{i+1} z_{i+1} \\ & + x x_{i+1}^2 z_{i+1} - x_i x_{i+1}^2 z_{i+1}\} \ln\left|\frac{x - x_i}{x - x_{i+1}}\right|. \end{aligned} \tag{8}$$

The quantities z_i are the derivatives calculated when constructing the spline [9], [10].

When x is large, it is usually advantageous to expand the integrand in (6) in powers of $1/x$ and then carry out the integration, thereby avoiding roundoff errors, which are dominant because of the strong cancellations that take place [7].

IV. Numerical Results and Discussion

In this section we apply Bode's integrals to calculate the susceptance of a wire antenna from its conductance. We assume a lossless wire antenna of length L fed at the center. The wire of diameter $2a$ is assumed lossless and radiating in free space.

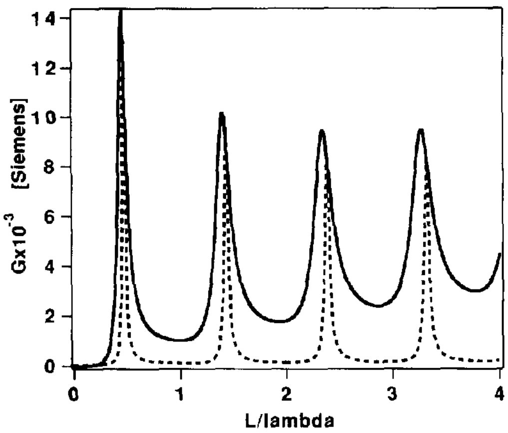

Fig. 1. Input conductance of a wire antenna as a function of L/λ_0. q = 11.11 (solid line) and q = 33.33 (dashed line).

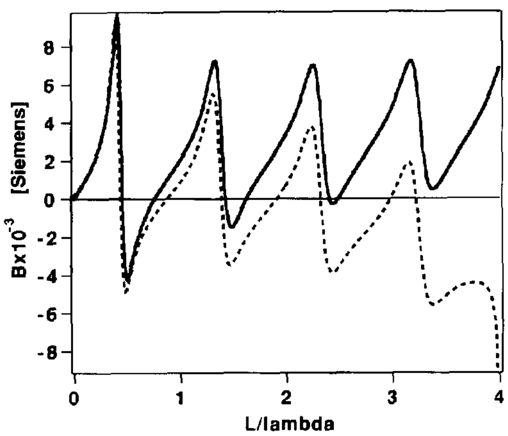

Fig. 2. Input susceptance of a wire antenna as a function of L/λ_0. q = 11.11. The solid line is the direct method-of-moments solution and the dashed line is obtained through Bode's integrals.

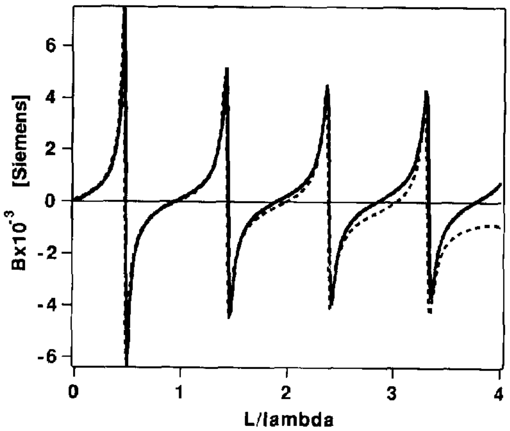

Fig. 3. Input susceptance of a wire antenna as a function of L/λ_0. q = 33.33. The solid line is the direct method-of-moments solution and the dashed line is obtained through Bode's integrals, where the conductance was calculated at 400 frequency points.

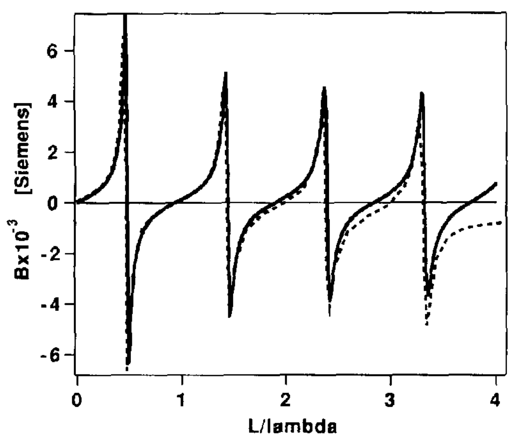

Fig. 4. Input susceptance of a wire antenna as a function of L/λ_0. q = 33.33. The solid line is the direct method-of-moments solution and the dashed line is obtained through Bode's integrals, where the conductance was calculated at 50 frequency points.

The method of moments is used to calculate the input admittance of the antenna as a function of frequency; the code was checked against the results presented by Harrington in [12]. Fig. 1 shows the input conductance of a dipole as a function of the ratio L/λ_0 for $L/2a$ = 74.2 (solid line, q = 11.11), and $L/2a$ = 10^4 (dashed line, q = 26.3). Our results for the case $L/2a$ = 74.2 agree with those in [12] to within the readability of the latter. The conductance was calculated at 400 frequency points in both cases. Fig. 2 shows the input susceptance calculated directly using the method of moments (solid line) and the one obtained through the present technique for $L/2a$ = 74.2. It is evident that the present method fails in the high frequency region but approximates the first resonance reasonably well. The origin of the discrepancy can be traced back to the fact that the integral in (1) extends over the entire real axis, which is not possible to incorporate into the present situation. The agreement improves rapidly if the real part is calculated over a wider range of frequencies. Despite this shortcoming, the method locates the first resonance reasonably well. For this case, where the peaks of the real part are not sharp, it is possible to approximate the real part over a wide range of frequencies without using a large number of points, thereby allowing the resonances to be more accurately located using the Bode's integrals. The agreement in susceptance is even much better when the peaks in the conductance are sharper, as shown in Fig. 3. The solid curve is the direct method-of-moments solution. Locating the zeros of the susceptance directly can be very time consuming. It is in this situation that the present method is most useful. As Fig. 3 shows, the resonances are located within plotting accuracy, even though the two curves are distinct over the region between the resonances and at the right edge of the plot. The sharper the peaks in the conductance, the better the agreement and consequently the more reliable the present method is. Our investigations have shown that for values of q larger than 15, the first resonant frequency is predicted within plotting accuracy if only the first peak in the input conductance is used, i.e., the range $0 \leq L/\lambda_0 \leq 1$ in Fig. 1.

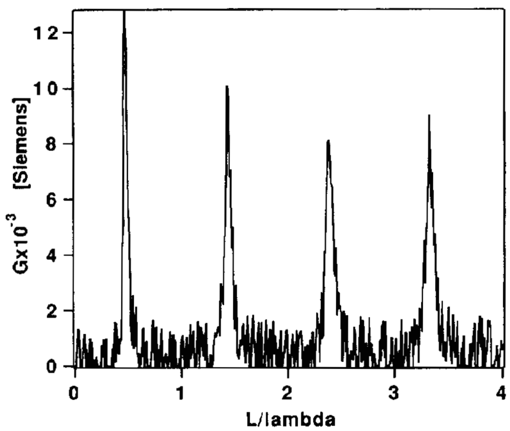

Fig. 5. Input conductance G of a wire antenna with $\pm$ 10% ($\pm 1.3\,\mathrm{mS}$) of noise superimposed. (Note that negative conductances are eliminated by setting the respective values to zero.)

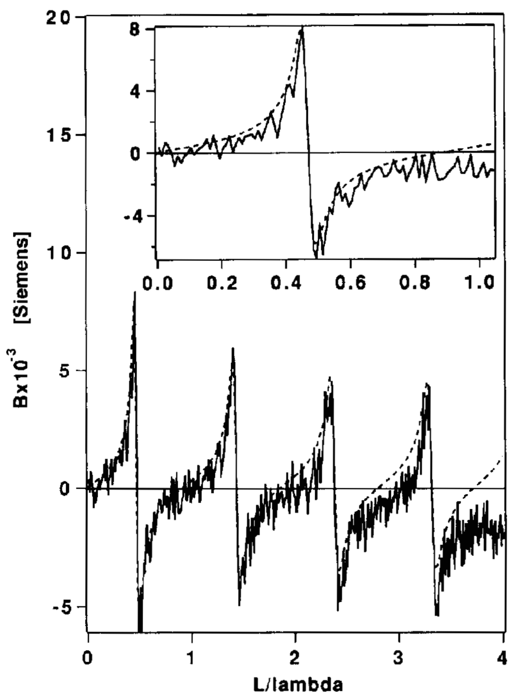

Fig. 6. Calculated input susceptance B corresponding to conductance of Fig. 5. The inset is the input susceptance calculated from only the first peak, $0 \leq L/\lambda_0 \leq 1$, of the conductance in Fig. 5.

It is worth pointing out that Bode's integrals allow an adequate description of the susceptance as long as the conductance is well described by the number of frequency points used. Fig. 4 shows the susceptance obtained from only 50 frequency points in the conductance (dashed line) and the method-of-moments solution (solid line) calculated at 400 points. It is clear that the differences between the dashed curve of Fig. 3, obtained from 400 points, and that from 50 points (dashed curve of Fig. 4) are minor, especially around the resonant frequencies; in other words, the presented example results in eight-fold reduction of required CPU time.

V. Noise Performance

Successful application of the present technique to calculate the input susceptance from measured profiles of the input conductance requires its stability to the errors inherently introduced by the measurement. To simulate these errors, random oscillations were superimposed on the calculated values of the conductance G. The oscillations represent a $\pm$ 10% random error in G.

Fig. 5 shows a plot of the corrupted real part of the input admittance for $q = 26.3$. Fig. 6 shows the calculated imaginary part using the corrupted real part. Clearly, the resonant frequencies are accurately, the susceptance satisfactorily, predicted despite the presence of the corrupting noise. The inset shows the imaginary part obtained from only one single peak of the noisy real part. The resonant frequency and susceptance are again satisfactorily predicted despite the presence of the random errors and the reduced number of frequency points.

VI. Conclusions

Since the real part of an antenna's input admittance versus frequency is usually a smoother function than the imaginary part, Bode's integrals are applied to significantly reduce computation times for admittance calculations. By using a cubic spline interpolation for the conductance in the numerical integration, the number of actual input admittance analyses can be reduced by at least a factor of eight—or even higher if the accuracy in the susceptance function is slightly sacrificed—while still satisfactory results are obtained for the resonances (zeros of susceptance). The algorithm is robust in the presence of random noise and can therefore be used to validate or improve measurements.

References

[1] H. W. Wyld, *Mathematical Methods for Physics*. New York: Addison-Wesley, 1976, ch. 12.

[2] N. Balabanian and T. A. Bickart, *Electrical Network Theory*. New York: Wiley, 1969, ch. 6.

[3] C. Kittel, *Introduction to Solid State Physics*. New York: Wiley, 1986, ch. 11.

[4] S. Amari, "Single-particle excitations of the electron gas," Ph.D. dissertation, Washington University, St. Louis, 1994.

[5] W. L. Stutzman and G. A. Thiele, *Antenna Theory and Design*. New York: Wiley, 1981.

[6] Z. Cai and J. Bornemann, "Rigorous analysis of radiation properties of lossy patch resonators on complex anisotropic media and lossy ground metallization," *IEEE Trans. Antennas Propagat.*, vol. 42, no. 10, pp. 1443–1446, Oct. 1994.

[7] S. Amari, "Evaluation of Cauchy principal-value integrals using modified Simpson rule," *Appl. Math. Lett.*, vol. 7, no. 3, pp. 19–23, 1994.

[8] J. M. Ziman, *The Principles of the Theory of Solids*. New York: Cambridge, 1972, ch. 8.

[9] W. H. Press *et al.*, *Numerical Recipes*. New York: Cambridge, 1986, ch. 3.

[10] W. Cheney and D. Kincaid, *Numerical Mathematics and Computing*. Monterrey, CA: Brooks/Cole, 1985.

[11] P. J. Davis and P. Rabinowitz, *Methods of Numerical Integration*. Orlando, FL: Academic, 1984.

[12] R. F. Harrington, *Field Computation by the Moment Methods*. Malabar, FL: Krieger, 1987, p. 72.